

Design & Simulation of Flexible Control For 3-phase Grid Connected Solar PV System

R.Srinivasan¹, C.R.Balamurugan², N.Shanmugasundaram³

¹Research scholar, Anna University, Chennai

²Department of EEE, Karpagam College of Engineering, Coimbatore

³Department of EEE, Vels Institute of Science Technology and Advanced Studies, Chennai, India

*Corresponding author E-mail: srinir.87@gmail.com

Abstract

A non-linear control progression for 3-stage (phase) lattice (grid) associated of PV generator is proposed here. This system is designed with PV arrays; grid filter; a voltage source inverter and a stimulating lattice or network. The regulator purposes are classified into three sections: i) making sure that the Most power point tracking (MPPT) are having photovoltaic boards, ii) assuring for power or control factor entity or unit in the grid plane iii) ensuring large-scale asymptotic constancy of the closed loop system. Lyapunov modelling approach is used by the controller and carried out by considering nonlinear model of the integral method. It is formally shown that the projected system controller congregates the scope of the objectives using a hypothetical constancy with stability analysis as well as simulation results.

Keywords: Solar PV System, DC link, 3-phase Inverter & converter.

1. Introduction

With intensifying concerns about unnatural changes in weather conditions and more in view of the fact that the previous spike in oil consequences where stopped to increase further, renewable power or energy, long measured a constructive appendage course. As of now the sources of lubrication and gasoline are still moderately economical. The worth of fossil fuels gets increased since the insufficiency of raw materials; rather the worth of renewable energy should get lowered because of technical growth and larger production series. And that is so the PV scheme gets becoming more brightened in the imminent years. The PV lattice associated systems became most significant applications in terms of solar energy (Chiang, 1998; Doncker, 2007; Enslin, 1991). Many surveys have been undertaken for various control stratagems of 3-phase grid connected PV elements in the last few years (Anthony Purcell, 2001; Cristian Lascu, 2000) All the same, fine incorporation of large PV system from the inverter requires extra functionality in the grid, like as reactive supremacy power. Therefore these new strategies of adding extra functions to the PV system may increase their average size and eliminates the chopper or direct chopper (DC-DC) converter that is more generally positioned among the photovoltaic inverter and generator. MPPT is replaced by the inverter for making simplicity augmentation as well as increases overall efficiency by reducing cost. Both features are presented in 3-phase inverter which is described at this juncture, adding together Perturb and Observe (P&O) MPPT procedure or algorithm. The proposed work is mainly focusing on the problem of power generation system i.e. power controlling of 3-stage lattice - connected in photo voltaic systems. A large-scale asymptotic constancy of complete control system with closed loop feature; MPPT realization for photovoltaic array; making sure of concord Power Factor (PF) for grid connection are the three major control or power objectives should be focused. These control or power managing purpose of the proposed work is to achieve the

above mentioned goals even there exists any climatic changes in regarding temperature and energy emission. At last, a nonlinear controller is produced utilizing Lyapunov plan procedure. A hypothetical examination is created to demonstrate the controller to identify whether it really congregates its targets by analyzing the originality that is affirmed by re-enactment. Work split up of this paper consists of: section II consists of modeled description about 3-stage lattice connected photovoltaic system. Section III depicts about designing and analysis of controller. Section IV illustrates mathematical simulation and controller monitoring performance.

2. System Depiction and Modeling

2.1. MPPT:

An MPPT algorithm is used to characterize the control strategy for extracting large energy from photovoltaic panel. Fundamentally, the outsized procedural families subsist: the family folks that search for the PPM by all-encompassing the power and voltage curve and the family that left over targets the PPM in a straight line. The family algorithms with cleaning purpose are to identify primary P&O as well as Incremental Conductance (INC) procedures. Perturb and Observe stays on the whole accepted and as a rule intuitive approach or method. This strategy outputs a rehashing arrangement of 3 stages: I) aggravate an underlying activity point by creating fluctuations in voltage and evaluates the forces when annoyance; ii) watch the power incline variations; iii) choose to change the voltage a similar way if the power variety is certain or the if control or power variety is negative then MPP approach is carried out. MPP should be applied for determining the sequence number that is to be carried out. Therefore the reference or operating point certainly not coincides with the MPP but merely fluctuates in the region of it. Modulating voltage amplitude is mandate for improving the performance of this

proposed technique by introducing some kind of intelligence methods using voltage variation. The mechanism cannot be applied over rapidly changing geological condition due to variations in power. Minimum number of sensors is necessary and an elaborated control circuit more if for getting the desired output. Instead of comparing powers in MPP, these techniques compare the instant and discrepancy conductance.

However, INC is developed using some heuristics which have been discussed earlier. The divergence exists between these techniques is that the power Vs voltage ratio. Here the point unswervingly sought the point that derivative power's voltage is zero. Finding procedure is based upon the sum value of conductance outputs. If the output of the sum value is optimistic (positive value) then operating point is left at MPP and variation's in the voltage level is obligatory. If the output of the sum is pessimistic (negative value), then the reference or operating point is left at the right of MPP and variations in pessimistic voltage value is done. Once the output of the sum reaches zero, then it is said to be MPP is achieved. The variations and the output are compared with P&O technique. Therefore it is confronted with the equivalent negotiation of region of MPP. The oscillation's amplitude and speed is measured approximately in the region of MPP, rather it precisely in case of rapidly varying economical or weather conditions. However a control circuit is required and makes this MPP more complex when compared to the PO algorithm.

2.2. System description:

The focal circuit of 3-stage lattice-associated photovoltaic scheme is revealed in Fig.1. The circuit is designed with photovoltaic arrays; a DC association capacitor 'C'; a 3-stage inverter (together with 6 highly supremacy power partial-conductors which guarantees a DC-AC control transformation as well as solidarity control aspect; an inductor channel L with its ESR obstruction r, and an electric lattice. Pulse width modulated signals are given as controlled inputs for the system and this is mentioned as *ua, ub* and *uc*; this input takes the value from the set {0, 1}. The grid or lattice voltages *ega, egb* and *egc* comprise a 3-phase objective system.

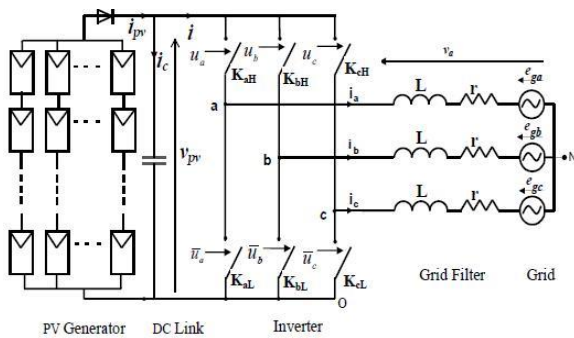


Fig.1: 3-phase grid connected PV system

2.3. PV array model:

A correspondent circuit for a PV cell is given in Fig. 2. The array model and its features with current characteristic being identified in many spaces (Ding, 2010; Doncker, 2007) and describes the following expression

$$I = I_{ph} - I_{sat} \left[\exp \left(\frac{q(V + IR_s)}{AkT} \right) - 1 \right] - \frac{V + IR_s}{R_p} \tag{1}$$

Where,

$$\begin{cases} I_{sat} = I_{satr} \left[\frac{T}{T_r} \right]^3 \exp \left[\frac{qE_{G0}}{Ak} \left(\frac{1}{T_r} - \frac{1}{T} \right) \right] \\ I_{ph} = [I_{phr} + K_I(T - 298)]\lambda \end{cases} \tag{2}$$

The distinctive standards of the constraints are given in (1) and (2) that can be recognised at many circumstances (Boldue, 1993; Bragard, 2010; Ertl, H. J, 2002), *A* is represented for diode ideal aspect, *k* represents Boltzmann constant and the value of *k* is equivalent to $1.3 \times 10^{-23} J / K$, *T* represents temperature on supreme scale in *K*, *q* is specified for its charge of electron and the value of *q* is $1.6 \times 10^{-19} C$ and \ddot{e} is the radiation in kW/m², *I_{phr}* is the short-trail current at 298 *K* and 1 kW/m², is the coefficient's of current temperature at *I_{phr}*, *E_{G0}* is the band gap for silicon, *Tr* = 302.18*K* is reference temperature, *I_{satr}* is cell saturation current at *Tr*. PV cluster comprises of *N_s* cells in arrangement shaped the board and of *N_p* boards in parallel as per the evaluated control required. The yield *v* and *I* can be known by the subsequent equations:

$$V_{pv} = N_s (V_d - R_s I) \tag{3}$$

$$I_{pv} = N_p I \tag{4}$$

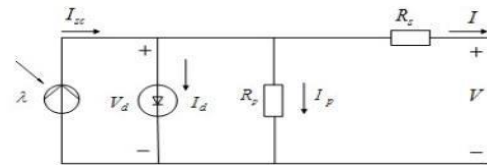


Fig.2 The equivalent circuit for a PV cell

PV originator measured here comprises of a few NU-183E1 modules. The relating electrical qualities of PV modules are appeared in Table I. Figure 3 and Figure 4 reveals that the related power and voltage (P-V) qualities gets varied under various conditions in temperature and radiation. This features the max power level M1 to M5 and the Table III describes their coordinates.

A chief descriptive feature of PV array is given in table II and it is specially modelled by means of Sharp NU-183E1 a component which is connected through an appropriate series-parallel with the mounted power of 71.75 kW. Since unavailability of chopper converter among the photovoltaic generator and inverter, photovoltaic cluster arrangement ought to be picked with the end goal that the yield voltage of the photovoltaic originator is adjusted with prerequisites of the inverter.

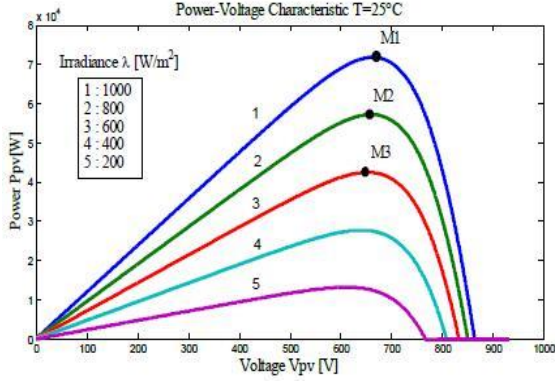
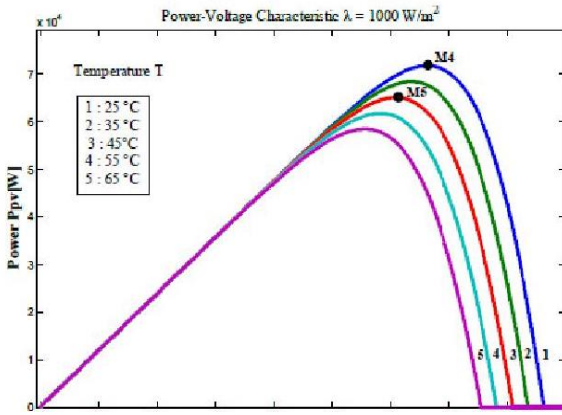
For this situation a 410V lattice has been picked, inverter would require no less than 570V DC transport keeping in mind the end goal to have the capacity to work accurately. The base number of modules associated in arrangement ought to be dictated by the estimation of the base DC transport voltage and the most pessimistic scenario economic conditions. Photovoltaic collection of array was established on the requirement of 28 series allied elements per string.

Table 1: Electrical stipulation for Solar Element NU-183E1

Parameter	Symbol	Value
Maximum Power	Pm	183 W
Short circuit current	Iscr	8.48 A
Open circuit voltage	Voc	31.1 V
Highest power voltage	Vm	29.9 V
Maximum power current	Im	7.66 A
Number of parallel modules	Np	1fvf
Number of series modules	Ns	48

Table 2: PV Array Specifications Using Sharpnu-183E1

Parameter	Symbol	Value
Total peak power	Pm	71.75 kW
Number of series strings	Ns	28
Number of parallel	Np	14
Number of PV panels	N	432
Voltage in maximum power	Vm	664
Current peak	Im	108 A

**Fig.3:** (P-V) description of photovoltaic Generator (NP=14 And NS=28) with unvarying heat and varying radiation**Fig.4:** (P-V) description of PV Generator (NP=14 and NS=28) with unvarying radiation and unstable temperature.**Table 3:** Maximum Power Points In Fig.3 And Fig.4

MPP	Vm [V]	Pm [KW]
M1	654.21	71.77
M2	651.04	57.21
M3	644.34	42.50
M4	654.21	71.77
M5	620.63	65.08

$$Q = \frac{3}{2} (e_{gq} i_d - e_{gd} i_q)$$

2.4. Modeling of 3-stage Lattice-Connected PV System

The condition-space representation of a 3-phase lattice or grid-associated photovoltaic structure is shown in Fig. 1 can be acquired by the dynamic conditions depicted as takes after:

$$\frac{d}{dt} \begin{bmatrix} i_a \\ i_b \\ i_c \end{bmatrix} = -\frac{r}{L} \begin{bmatrix} i_a \\ i_b \\ i_c \end{bmatrix} + \frac{v_{pv}}{3L} \begin{bmatrix} 2 & -1 & -1 \\ -1 & 2 & -1 \\ -1 & -1 & 2 \end{bmatrix} \begin{bmatrix} u_a \\ u_b \\ u_c \end{bmatrix} - \frac{1}{L} \begin{bmatrix} e_{ga} \\ e_{gb} \\ e_{gc} \end{bmatrix} \quad (5a)$$

$$\frac{d}{dt} v_{pv} = \frac{1}{C} i_{pv} - \frac{1}{C} (u_a i_a + u_b i_b + u_c i_c) \quad (5b)$$

The instantaneous model in d-q frame can be acquired by implementing d-q transformation
Where,

$$u_i = \begin{cases} 1 \rightarrow K_{iH} : on; K_{iL} : off \\ 0 \rightarrow K_{iH} : off; K_{iL} : on \end{cases}$$

By using d-q transformation to (5a-b), one acquire the subsequent instantaneous replica in d-q frame

$$\frac{d}{dt} i_d = -\frac{r}{L} i_d + \omega i_q + \frac{v_{pv}}{L} u_d - \frac{1}{L} e_{gd} \quad (6a)$$

$$\frac{d}{dt} i_q = -\frac{r}{L} i_q - \omega i_d + \frac{v_{pv}}{L} u_q - \frac{1}{L} e_{gq} \quad (6b)$$

$$\frac{d}{dt} v_{pv} = \frac{1}{C} i_{pv} - \frac{1}{C} (u_a i_a + u_b i_b + u_c i_c) \quad (6c)$$

Where,

$$\begin{aligned} \begin{bmatrix} i_{dqo} \end{bmatrix} &= \begin{bmatrix} T_{abc}^{dqo} \end{bmatrix} \begin{bmatrix} i_{abc} \end{bmatrix} ; \begin{bmatrix} e_{gdqo} \end{bmatrix} = \begin{bmatrix} T_{abc}^{dqo} \end{bmatrix} \begin{bmatrix} e_{gabc} \end{bmatrix} \\ T_{abc}^{dqo} &= \frac{2}{3} \begin{bmatrix} \sin(\omega t) & \sin(\omega t - \frac{2\pi}{3}) & \sin(\omega t - \frac{4\pi}{3}) \\ \cos(\omega t) & \cos(\omega t - \frac{2\pi}{3}) & \cos(\omega t - \frac{4\pi}{3}) \\ \frac{1}{2} & \frac{1}{2} & \frac{1}{2} \end{bmatrix} \end{aligned}$$

$$\begin{bmatrix} u_{dqo} \end{bmatrix} = \begin{bmatrix} T_{abc}^{dqo} \end{bmatrix} \begin{bmatrix} u_{abc} \end{bmatrix}$$

The transformation matrix is given by

$$P = \frac{3}{2} (e_{gd} i_d + e_{gq} i_q) \quad (8)$$

Where P is dynamic power and Q is spontaneous power. In synchronous d-q rotating, $e_q = 0$, consequently

$$P = \frac{3}{2} e_{gd} i_d \quad (9a)$$

$$Q = -\frac{3}{2} e_{gd} i_q \quad \text{And} \quad (9b)$$

Dynamic power P can be regulated by i_d and spontaneous power Q can be regulated by i_q .

3. Controller Design and Analysis

In order to design an appropriate or outline a proper control for the system (6) that is depicted in earlier section, includes the control goals, plan for control design and constancy examination will be

analysed, by considering the account of nonlinear attribute and the Many-Input and Many-Output (MIMO) framework or phase of the system

3.1. Control objectives

For defining the system control strategies it is necessary to define the objectives of control design or plan at earlier and this can be originated as follows:

- i) Photovoltaic arrays with MPPT,
- ii) Grid's union PF,
- iii) Asymptotic constancy of entire model.

3.2. Nonlinear control design

A Lyapunov dependent control with nonlinear characteristics is proposed once if the destinations are characterized, as the multi input multi output framework is profoundly nonlinear. The principal objective is to uphold genuine power P to follow up or monitor the most extreme power point PM. It's as of now carry, the power can be forbidden by d-pivot current 'id'. The MPPT calculation in view of the P&O procedure [11] is turned to create the indication flag idref of the present id hence if "id = idref" the dynamic power P tracks it's most extreme esteem i.e. P=PM.

The error to be introduced first

$$e_1 = i_d - i_{dref} \tag{10}$$

So as to accomplish the MPPT objective, one can look for that the blunder e1 is diminishing. Therefore, the dynamic of e1 must be unmistakably characterized at the end. Originating (10), it follows from (6a) that:

$$\dot{e}_1 = -\frac{r}{L}i_d + \omega i_q + \frac{v_{pv}}{L}u_d - \frac{1}{L}e_{gd} - \dot{i}_{dref} \tag{11}$$

The goal, now, is to make e1 eventually fading by construction of obligatory to behave as follows

$$\dot{e}_1 = -c_1 e_1 \tag{12}$$

Where $c1 > 0$ depicts a modelling factor, Equations (11) and (12) combinable produces in charge of law,

$$u_d = \frac{L}{v_{pv}} \left(-c_1 e_1 + \frac{r}{L}i_d - \omega i_q + \frac{1}{L}e_{gd} + \dot{i}_{dref} \right) \tag{13}$$

The second control target implies that the lattice streams ia, ib and ic ought to be sinusoidal. The AC matrix voltage stage exists with ega, egb and egc separately. In sequence the receptive power becomes invalid. As per (9b) the reference current iqref of iq ought to be zero (iqref = 0). The second after mistake is then presented,

$$e_2 = i_q - i_{qref} \tag{14}$$

Its derivative, using (6b), is

$$\dot{e}_2 = -\frac{r}{L}i_q - \omega i_d + \frac{v_{pv}}{L}u_q - \frac{1}{L}e_{gq} \tag{15}$$

So as to accomplish a power aspect, the mistake vanishes exponentially. This adds up to authorizing its subsidiary to carry on as takes after

$$\dot{e}_2 = -c_2 e_2 \tag{16}$$

Where $C2 > 0$ being a modelling constraint, equations (15) and (16), combinely produces II control law as follows

$$u_q = \frac{L}{v_{pv}} \left(-c_2 e_2 + \frac{r}{L}i_q + \omega i_d + \frac{1}{L}e_{gq} \right) \tag{17}$$

Since the two control laws such as ud and uq are obviously characterized, the worry currently is to guarantee that the steadiness of the shut circle is completely guaranteed.

3.3. Stability analysis

The goal of the worldwide dependability of shut circle framework would now be able to be investigated. This can be completed by watching that the proposed controllers balance out the entire framework with the state vector (e1, e2). Accompanying quadratic Lyapunov work is considered

$$V = \frac{1}{2}e_1^2 + \frac{1}{2}e_2^2 \tag{18}$$

Its derivative using (12) and (16) is obtained as follows

$$\dot{V} = -c_1 e_1^2 - c_2 e_2^2 \tag{19}$$

Which implies that ≤ 0 and thus demonstrates that the symmetry balances over (e1, e2) = (0,0) of the shut circle framework with the state vector (e1,e2) is internationally asymptotically steady (GAS) [12]. This equally implies, for whenever t0, and whatever the underlying conditions (e1 (t0), e2 (t0)).

3.4. Proposition

Closed-loop system is considered and the system of Fig.1 is represented by its nonlinear model (5a-b), and then the propositions are as follows;

- i) GAS is a closed loop method.
- ii) The monitoring error e1 gets cleared exponentially by involving MPPT accomplishment.
- iii) The error e2 congregated to zero by applying the power aspect unit or ratio.

4. Simulation Results

The hypothetical exhibitions of the projected controller with nonlinear characteristics are currently represented by re-enactment. The trial setup depicted in Fig.5, is recreated utilizing SIMULINK tool using MATLAB. The infused streams to the matrix must be coordinated with the framework voltages. A stage bolted circle is utilized. The features of the forced system are listed for the reference.

The controller constraint that is used is mentioned in Table V. However the constraints have certain 'trial-and error' search method and that is selected to be apt. Fig.6 shows the PO block-diagram and implementation which generates idref. The ensuing loop be in charge of concerts are illustrated by Fig.7 to Fig.12.

Table 4: Comptroller parameter

Parameter	Symbol	Value
Photovoltaic array	PV power	70kW
DC link capacitor	C	3300µF
Grid filter inductor	L, r	3mH 0.2Ω
PWM	Toggle Frequency	10kHz
Grid	AC source Line frequency	220V 50Hz

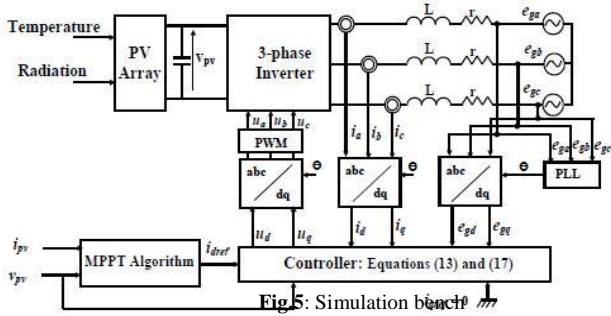


Fig.5: Simulation block

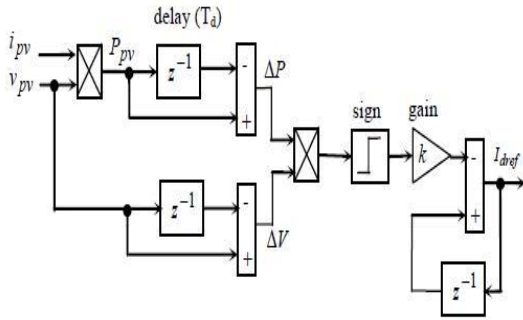


Fig.6: PO algorithm performance using Simulink tool

Table 5: Comptroller parameter

Parameter	Symbol	Value
Design parameters	c1	105
	c2	4×104
P&O algorithm Parameters	Delay time Td	10-4
	Step value k	0.3

4.1. Transform effect

Fig.7 demonstrates the ideal MPPT within sight of energy tread variations in the interim, the heat constraint is kept steady, correspondent to 27 °C. The re-enacted energy profile is: an initial step change is performed somewhere in the range of 700 and 1050W/m2 at t =0.6s then the next process occurs somewhere in the range of 1050 and 750W/m2 at time t =0.8s. The figure demonstrates that the PV control caught shifts somewhere in the range and after those profits to (57.2kW). These qualities compare (refer Fig.3) to most extreme focuses M decreasing series of the bends related to the thought about radiation, individually. The figure additionally demonstrates that the voltage of the PV exhibit Vpv shifts between Vpv = 654.3V and Vpv = 668.2V and afterward comes back to 659V, which compare extremely relies with ideal voltages. Fig. 8 demonstrates infused streams ia and the network voltage ega. This figure obviously demonstrates that the network current is sine function and in stage with the lattice voltage ega, demonstrating that unit of factor is accomplished. The substituting stream of the grid is illustrated by Fig.9.

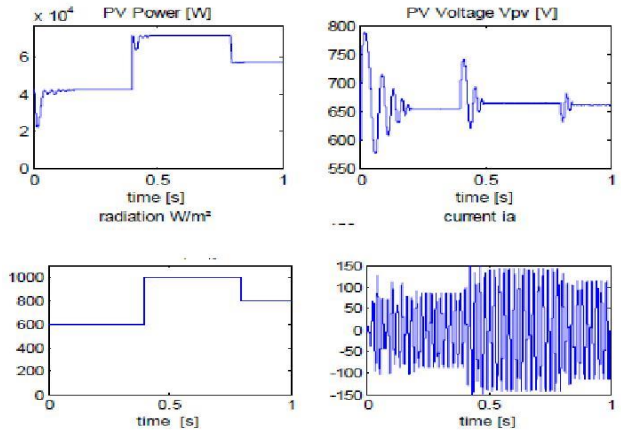


Fig.7: MPPT capability controller with variations in radiation changes.

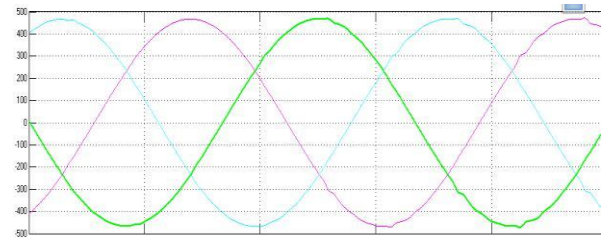


Fig 8. Injection of voltage to Grid

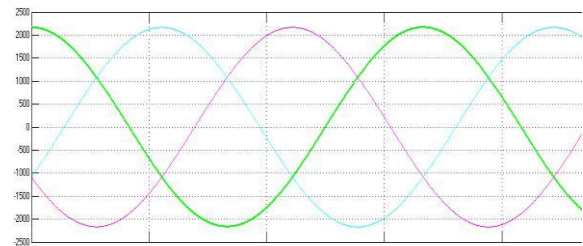


Fig 9. Current injected to Grid

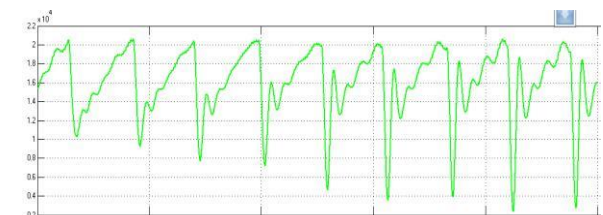


Fig 10. Current injected to Grid Active power supplied to grid

5. Conclusions:

The paper concludes that the function of 3 stage inverter has been implemented and regulated successfully. The fundamental component of the displayed framework doesn't involve a halfway phase of chopper control, as the extreme power is fixed up by inverter itself by methods for P&O calculation. The framework flow has been depicted based on nonlinear characteristics of state-space display (5a-b). In light of a changed model, a non-linear regulator characterized by (13) and is composed and broke down utilizing a Lyapunov model. The regulator destinations are described in triple: i) guaranteeing the MPPT of photovoltaic generator; ii) ensuring a supremacy control consider the unit of the framework iii) guaranteeing worldwide asymptotic strength of shut circle framework. Utilizing both formal examination and re-enactment, it has been demonstrated that controller meets every one of the targets.

The instigator can inscribe the termination as an entire in a section or by building up the points. An illustration is given as under.

- 1) Cooling derivatives bend can be utilized to comprehend the little changes in the under cooling of the fluids and solidus temperature.
- 2) Warm investigation is a decent method to control carbides, shrinkage and miniaturized scale shrinkage arrangement.
- 3) It is unmistakably demonstrated that there is noteworthy decrease in under cooling degree on the combinations and the estimation of vaccination file was expanded. In spite of the fact that the expansion of Al,Ca,Zr-FeSi pre-conditioners gives no huge impact.
- 4) The utilization of relative execution makes an unmistakable qualification of the composites effectiveness and could be inferred that inoculants like S, Ca, O are immunized iron gave the most impact.
- 5) From the outcome acquired, it could be found relatively that the inoculants give the best effectiveness taken after by Ca, Zr-FeSi and Ca, Ba-FeSi inoculants separately.

References

- [1] Barrade, P. Delalay, S. & Rufer A. (Apr. 2012), Direct connection of super capacitors to photovoltaic panels with on-off maximum power point tracking," IEEE Trans. Sustainable Energy, vol. 3, no. 2, pp. 283–294.
- [2] Benavidas N. & Chapman, P., (Nov. 2005), Power Electron., vol. 20, no. 6, pp. 1303–1309.
- [3] Boldue, P., Lehmicke, D. & Smith, J., (1993) Performance of a grid connected PV system with Energy storage, in Proc. IEEE Photovoltaic Spec. Conf., pp. 1159–1162.
- [4] Bragard, M., Soltau, N., Doncker, R. W. D. & Schiemgel, A. (April 2010) Design and implementation of a 5 kW photovoltaic system with Li-ion battery and additional dc/dc converter, in Proc. IEEE Energy Convers. Congr. Expo., pp. 2944–2949.
- [5] Chiang, S. J., Chang, K. T. & Yen, C. Y., (Jun 1998) Residential photovoltaic energy storage system, IEEE Trans. Ind. Electron., vol. 45, no. 3, pp. 385–394.
- [6] Ding, F., Li, P., Huang, B., Gao, F., Ding, C. & Wang, C. (2010), Modeling and Simulation of grid connected hybrid PV/battery distributed generation system, in Proc. China Int. Conf. Electr. Distrib., pp. 1–10.
- [7] Doncker, R. W. D., Meyer, C., Lenke, R. U. & Mura, F. (Nov 2007), Power Electronics for future utility applications, in Proc. IEEE 7th Int. Conf. Power Electron. Drive Syst., pp. K-1–K-8.
- [8] Enslin, J. H. & Snyman, D. B., (Jan 1991), Combined low-cost, high efficient inverter, peak power tracker and regulator for PV applications, IEEE Trans. Power Electron., vol. 6, no. 1, pp. 73–82.
- [9] Ertl, H. J., Kolar, W. & Zach, F., (Oct. 2002) A novel multi cell dc-ac converter for applications in renewable energy systems, IEEE Trans. Ind. Electron., vol. 49, no. 5, pp. 1048–1057.
- [10] Ho, C., Breuninger, H., Pettersson, S., Escobar, G., Serpa, L. & Coccia, A., (Jun. 2012), Practical design and implementation procedure of an interleaved boost converter using SiC diodes for PV applications, IEEE Trans. Power Electron., vol. 27, no. 6, pp. 2835–2845.
- [11] Hu, Y., Tatler, J. & Chen, Z., (Aug. 2004), bidirectional DC/DC power electronic converter for an energy storage device in an autonomous power system, in Proc. IEEE Power Electron. Motion Control Conf., pp. 171–176.
- [12] Auzani Jidin, Nik Idris, Mohamed Yatim, (Sept Oct 2011), Simple Dynamic Over modulation Strategy For Fast Torque Control in DTC of Induction Machines With Constant-Switching-Frequency Controller IEEE transactions on industry applications, Vol. 47, No. 5.
- [13] Anthony Purcell, P. Acarnley, (May 2001.) Enhanced Inverter Switching for Fast Response Direct Torque Control, IEEE Transactions on Power Electronics, Vol. 16, No. 3
- [14] A. Mishra, P. Choudhary, (December 2012), Speed Control Of An Induction Motor By Using Indirect Vector Control Method, IJETAE, Volume 2, Issue 12.
- [15] B. K. Bose. (1997), Power Electronics and Variable Frequency Drives. IEEE Press, New York.
- [16] Cristian Lascu, Boldea, Blaabjerg, A. (Feb 2000.) Modified Direct Torque Control for Induction Motor Sensorless Drive, IEEE transaction on Industry Applications, Vol. 36, No. 1.
- [17] E. Bassi, P. Benzi, S. Buja, (Oct. 1992) A Field Orientation Scheme for Current-Fed Induction Motor Drives Based on the Torque Angle Closed-Loop Control, IEEE Transactions on Industry Applications, Vol. 28, No. 5, Sept.
- [18] Ehsan Hassankhan, Davood A. Khaburi, (2008), DTC-SVM Scheme for Induction Motors Fed with a Three-level Inverter, World Academy of Science, Engineering and Technology.
- [19] Giovanna Oriti and Alexander L. Julian, (August 2011.) Three-Phase VSI with FPGA-Based Multisampled Space Vector Modulation, IEEE transactions on industry applications, Vol. 47, No. 4.
- [20] H. Arabaci and O. Bilgin, (June 2012), Squirrel Cage of Induction Motors Simulation via Simulink, International Journal of Modeling and Optimization, Vol. 2, No. 3.
- [21] C.R. Balamurugan, "Three Area Power System Load Frequency Control Using Fuzzy Logic Controller" International Journal of Applied Power Engineering, ISSN No. 2252-8792, vol. 7, no. 1, pp. 18-26, April 2018.
- [22] C.R. Balamurugan, R. Bensraj, "Analysis of Various Carriers Overlapping PWM Strategies for a Single Phase Ternary Multilevel Inverter" International Journal of Applied Power Engineering, ISSN No. 2252-8792, vol. 7, no. 1, pp. 27-39, April 2018.
- [23] C.R. Balamurugan, K. Vijayalakshmi, "Comparative Analysis of Various Z-source Based Five Level Cascaded H-bridge Multilevel Inverter" Bulletin of Electrical Engineering and Informatics, ISSN No. 2302-9285, vol. 7, no. 1, pp. 1-14, March 2018.
- [24] R. Umamageswari, C.R. Balamurugan, T.A. Ragavendiran, "Selective Harmonics Mitigation Modulation Scheme Applied to CHB and NPC Multilevel Inverters", Journal of Electrical Engineering, ISSN No: 1582-4594, Vol. 18, No. 2, pp. 1-8, June 2018.
- [25] C.R. Balamurugan, A.N. Abhirami, "Z Source Fed H-Type Diode Clamped Multilevel Inverter", Journal of Advanced Research in Dynamical and Control Systems, ISSN 1943-023X, Special Issue : 17, Nov 2017, pp. 1785-1794.